

Effect of Zr^{+4} ion substitution on the structural, dielectric and electrical properties of $Sr_5LaTi_3Nb_7O_{30}$ ceramics

M. R. RANGA RAJU, R. N. P. CHOUDHARY*

Department of Physics and Meteorology, I. I. T. Kharagpur 721 302, India

E-mail: crnpfl@phy.iitkgp.ernet.in

Polycrystalline Zr-modified $Sr_5LaTi_3Nb_7O_{30}$ compound was prepared by a high-temperature solid-state reaction technique. X-ray structural analysis confirmed the formation of compound in an orthorhombic system at room temperature. Detailed studies of the dielectric parameters (dielectric constant and tangent loss) as a function of frequency (1–100 kHz) at different temperature (150 to 650 K) were carried out. It was found that as Zr^{+4} concentration increases in $Sr_5LaTi_{3-x}Zr_xNb_7O_{30}$, the value of dielectric constant decreases. These compounds show ferroelectric-paraelectric phase transition of diffuse type at 283, 305 and 320 K for $x = 0, 1$ and 2 respectively. The transition temperature (T_c) shifts towards higher temperature and maximum dielectric constant value (ϵ_{max}) decreases with increasing Zr^{+4} concentration for $x = 0$ to $x = 2$. When Ti^{+4} cations were completely replaced by Zr^{+4} cations (i.e., $Sr_5LaZr_3Nb_7O_{30}$), the compound does not show any phase transition. Impedance-spectroscopic studies provided an insight into the electrical properties and understanding of relaxation behavior of the material. Measurement of electrical conductivity as a function of temperature suggests that the compounds have a negative temperature coefficient of resistivity (NTCR) with a typical semiconductor behavior. © 2004 Kluwer Academic Publishers

1. Introduction

From the first report of ferroelectricity in $BaTiO_3$ [1], there has been an increasing interest in developing and searching new ferroelectric oxides for the device applications, which led to the discovery of numerous ferroelectric materials. During the process, a large number of ferroelectric oxides of different structural families such as perovskite, spinel, tungsten-bronze (TB) etc., have been discovered. Some of the ferroelectric niobates of TB structure have excellent properties such as pyroelectric, electro-optic, photorefractive, piezoelectric etc. [2–6] useful for device applications. The TB structure consists of a skeleton framework of BO_6 octahedra sharing corners to form three different types of tunnels parallel to the c -axis in the unit cell of a general formula $(A_1)_4(A_2)_2(C)_4(B_1)_2(B_2)_8O_{30}$ [7]. There are 12-coordinated A_1 site and 15-coordinated A_2 site corresponding to four-fold and five-fold tunnels respectively. The 9-coordinated c -site has the smallest space among all and generally the smallest interstice c is empty. There is a scope for variety of cations (i.e., of different ionic radius and valency) substitution at the many available interstitial sites (i.e., A_1, A_2, B_1 and B_2) that can tailor physical properties/device parameters. Therefore, they possess many interesting properties like electro-optical, pyroelectric, piezoelectric, etc. at room temper-

ature. Recently we are in search of new materials for many electronic applications. In order to find some new tungsten-bronze niobate ceramics, some work has been carried out in quaternary systems such as $BaO-Nd_2O_3-TiO_2-Nb_2O_5$ system [8], Shannigrahi and Palai [9, 10] reported some interesting work on $Ba_5RTi_3Nb_7O_{30}$ ($R = Dy, Sm$) and $Ba_4R_2Ti_4Nb_6O_{30}$ ($R = Y, Sm$ and Dy). Singh *et al.* [11] reported effect of Zr on physical properties of $Ba_5YTi_{3-x}Zr_xNb_7O_{30}$ ($x = 0, 1, 2$ and 3) compounds. Recently Zheng *et al.* [12] reported crystal structure and dielectric properties of $BaO-Sm_2O_3-TiO_2-Nb_2O_5$ system. Detailed literature survey shows that not much work on the titled compounds have been reported so far. In this work we have attempted to synthesize a group of compounds of TB-structural family of a general formula $Sr_5LaTi_{3-x}Zr_xNb_7O_{30}$ ($x = 0, 1, 2$ and 3) using a high-temperature solid-state reaction technique. In this article we report the effect of Zr^{+4} cations substitution (at the Ti sites) on the structural, dielectric and electrical properties of the titled compound.

2. Experimental

Polycrystalline samples of $Sr_5LaTi_{3-x}Zr_xNb_7O_{30}$ ($x = 0, 1, 2$ and 3) were prepared by a high-temperature

*Author to whom all correspondence should be addressed.

solid-state reaction technique using high purity raw materials: SrCO₃ (99.9%, M/s B. D. H Chemicals), La₂O₃ (99.9%, M/s Indian Rare-Earth Ltd.), TiO₂ (99.9%, M/s s.d. Fine Chemicals Ltd.), ZrO₂ (M/s Aldrich Chemicals, USA) and Nb₂O₅ (99.9%, M/s Loba Chemie. Co. India) in suitable stoichiometry. The mixtures of the ingredients were thoroughly mixed and ground in wet medium (methanol) for 1 h, and in dry condition for 1 h in an agate mortar and pestle. Calcination was carried out in a high purity alumina crucible at 1150°C for 15 h in an air atmosphere. The process of calcination and mixing was repeated (twice) to confirm the formation of the compound. To check the formation of the compounds and to obtain the crystal structure, XRD spectra were taken over a wide range of Bragg angles ($20^\circ \leq 2\theta \leq 60^\circ$) on calcined powder at room temperature using a Philips (PW 1710) X-ray diffractometer (Cu K α radiation, $\lambda = 0.15418$ nm). The fine and homogeneous powders of the Sr₅LaTi_{3-x}Zr_xNb₇O₃₀ ($x = 0, 1, 2$ and 3) compounds were mixed with polyvinyl alcohol (PVA as a binder) to reduce the brittleness, and compacted into cylindrical pellets of 10 mm diameter and 1–2 mm thickness by applying a uniaxial pressure of 6 Mpa in a hydraulic press. The pellets were sintered at 1200°C for 15 h in an air atmosphere using an alumina crucible. The organic binder (PVA) was burnt out during the process of high temperature sintering. The sintered unpolished flat surface of the pellet was gold coated by a sputtering technique to check the surface morphology of the pellet. The surface morphology of the pellet was studied by scanning electron microscopy (SEM, Jeol JSM-5800). For electrical characterizations, the flat and clean surfaces of the pellet were painted with high-purity air-drying conducting silver paste. The dielectric and electrical conductivity (i.e., impedance-spectroscopy study) was studied on the sintered pellets of the compound and the data were recorded using a computer-controlled HIOKI 3532 LCR Hitester along with a laboratory-made sample-holder and heating arrangement over a wide range of temperature at

TABLE I Comparison of lattice parameters a , b and c (nm), volume (nm³), average crystallite size D (nm) and other related dielectric data of the Sr₅LaTi_{3-x}Zr_xNb₇O₃₀ ($x = 0, 1, 2$ and 3) compounds. The estimated standard deviation in lattice parameters is about ± 0.0020 Å

Parameters	$x = 0$	$x = 1$	$x = 2$	$x = 3$
a	1.4462	1.4514	1.4561	1.4584
b	0.8026	0.8039	0.8077	0.8103
c	1.1293	1.1314	1.1407	1.1387
V	1.3108	1.3201	1.3416	1.3457
D	28	41	44	37
E_a (eV)	1.87	1.79	1.43	1.13
γ	1.21	1.50	1.85	–
δ_g	84	92	96	–
T_c (K)	283	305	320	–
ϵ_{\max}	531	375	275	–
ϵ_{RT}	514	375	271	171
$\tan \delta_{RT}$	0.011	0.032	0.045	0.045
$\tan \delta_{T_c}$	0.024	0.032	0.045	–

a dc signal of 1.3 V. Chromel-alumel thermo-couple and AGRONIC-161 digital millivoltmeter were used to measure the temperature.

3. Results and discussion

3.1. Structural and microstructure analysis

The XRD patterns of all the four compounds Sr₅LaTi_{3-x}Zr_xNb₇O₃₀ ($x = 0, 1, 2$ and 3) were sharp with single diffraction peak, which were different from that of the ingredients. The diffractogram of all the compounds is compared and found almost similar (Fig. 1). All the observed peaks (reflections) were indexed in the tetragonal and orthorhombic crystal system using a standard computer package POWDMULT [13]. Finally an orthorhombic unit cell of the compound was selected on the basis of a good agreement between observed and calculated d values. The crystallite size of the samples was calculated from the peak width ($\Delta 2\theta_{1/2}$) and peak position of reflections using the Debye-Scherrer relation [14] and the calculated values are given in Table I.

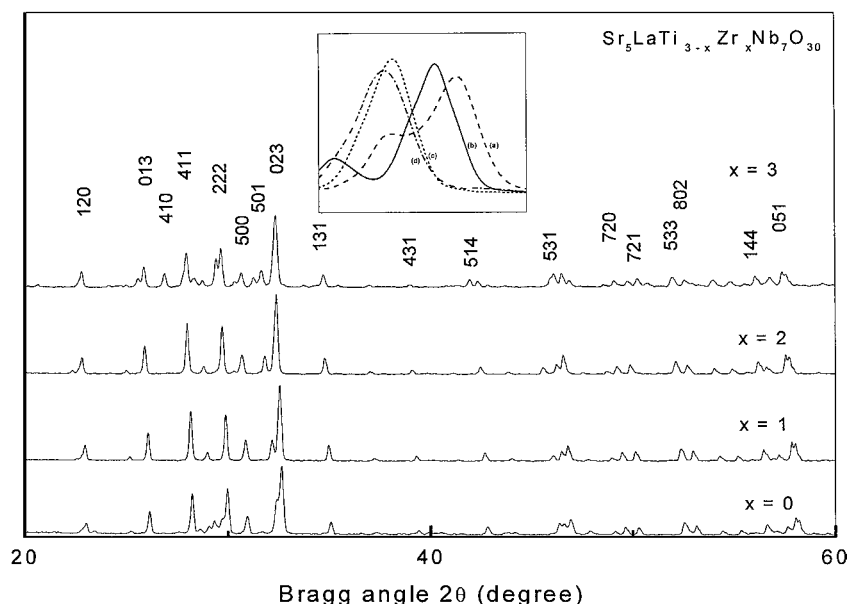


Figure 1 Comparison of X-ray diffraction profile for Sr₅LaTi_{3-x}Zr_xNb₇O₃₀ ($x = 0, 1, 2$ and 3) recorded at room temperature. The (023) peak corresponding to $x = 0, 1, 2$ and 3 is reproduced in (a), (b), (c) and (d) in an expanded 2θ scale, is shown in the inset.

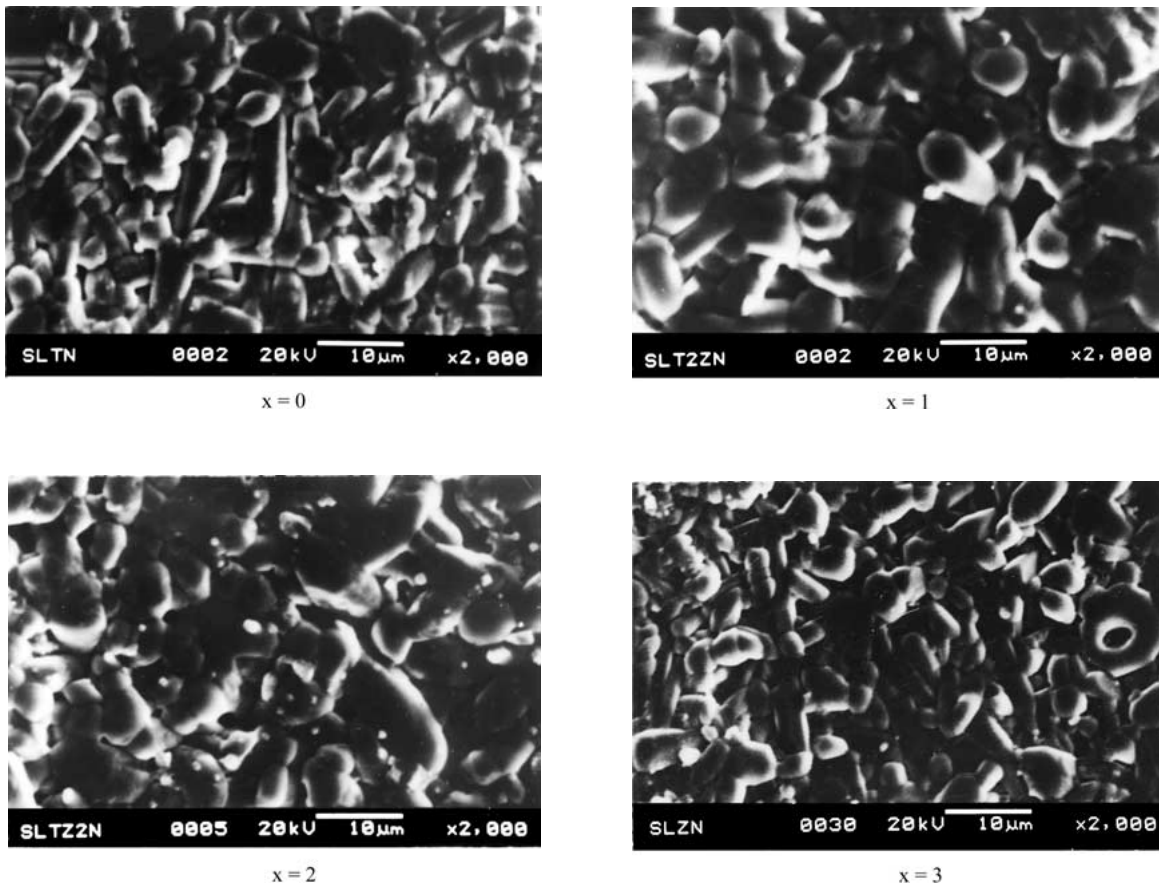


Figure 2 SEM micrographs of $\text{Sr}_5\text{LaTi}_{3-x}\text{Zr}_x\text{Nb}_7\text{O}_{30}$ ($x = 0, 1, 2$ and 3).

As the powder samples were taken to record XRD pattern, the broadening due to strain, beam divergence and other effects were ignored. The variation in the crystallite size can be well demonstrated by the variation in $\Delta 2\theta_{1/2}$ in (023) reflection measured at an expanded 2θ -scale is shown in the inset of Fig. 1. A small change in the unit cell volume of these compounds as a function of x may be due to the distribution of the cations of different ionic size ($\text{Ti} = 0.68 \text{ \AA}$ and $\text{Zr} = 0.79 \text{ \AA}$) at the B-interstitial sites. This is well supported by the observation of a significant variation in the relative intensities of (120), (222), (431), (531) and (802) reflections.

The quality of the sintered pellets and distribution of the grains over the sample surface were studied by scanning electron microscopy. The SEM micrographs (Fig. 2) show nearly uniform distribution of the grains on the sample surface. Most of the grains were found to be spherical in shape along with some grains of columnar shape, which may be due to the presence of some liquid phase during the high temperature sintering process. The grains size is varying from 1–10 μm . The average grain size was determined by the linear intercept method and was found to be in the range of 3.5–4.5 μm . The bulk density (d_{exp}) of the sintered sample was calculated using the conventional physical method and found to be 4.46, 4.58, 4.57 and 4.65 g/cc for $x = 0, 1, 2$ and 3 respectively. The theoretical density (d_{theo}) of the sample was found to be 4.69, 4.77, 4.79 and 4.89 g/cc, with $x = 0, 1, 2$ and 3 respectively. The

average experimental density of the samples was found to be more than 95% of the theoretical density.

3.2. Dielectric properties

The variation of ϵ and $\tan \delta$ at room temperature with frequency (1 to 100 kHz) is shown in Fig. 3. It was observed that in the low frequency range, the ϵ decreases with increasing frequency exhibiting the typical characteristic of a polar dielectric material. At higher frequencies, ϵ becomes almost frequency independent.

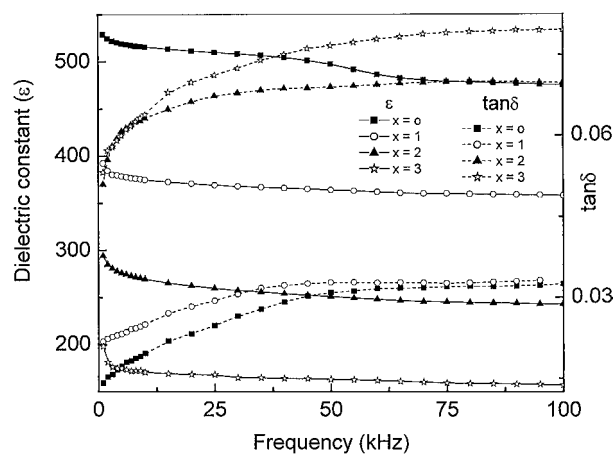


Figure 3 Frequency dependence of ϵ and $\tan \delta$ of $\text{Sr}_5\text{LaTi}_{3-x}\text{Zr}_x\text{Nb}_7\text{O}_{30}$ ($x = 0, 1, 2$ and 3).

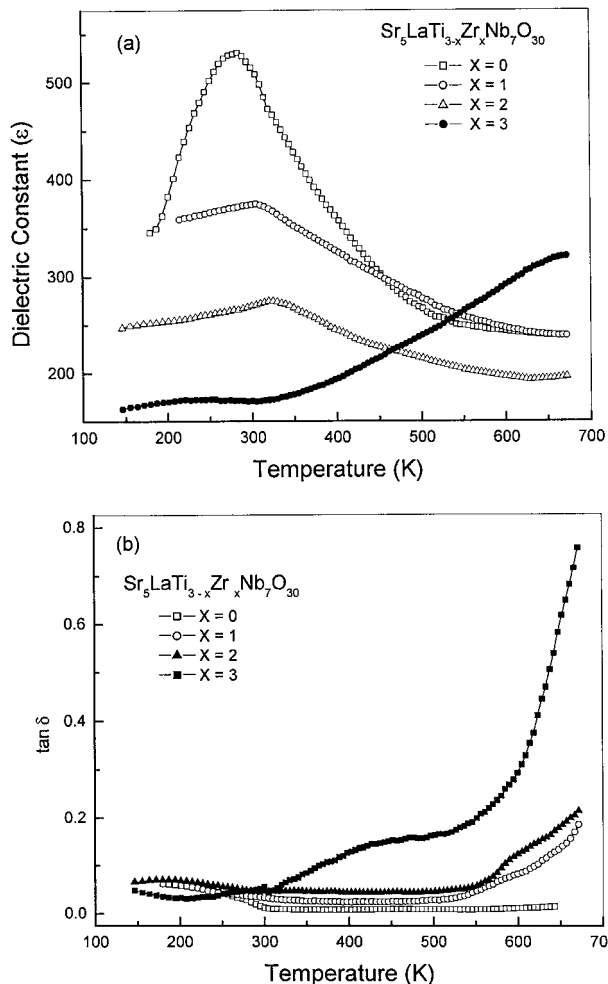


Figure 4 Variation of (a) ϵ and (b) $\tan \delta$ of $\text{Sr}_5\text{LaTi}_{3-x}\text{Zr}_x\text{Nb}_7\text{O}_{30}$ ($x = 0, 1, 2$ and 3) with temperature.

The $\tan \delta$ value increases slowly at lower frequencies, but at higher frequencies it becomes almost constant and frequency independent, which is a typical behavior of the dielectrics.

The temperature variation of ϵ and $\tan \delta$ of all the four compounds were shown in Fig. 4a and b respectively. It was observed that the compounds with $x = 0, 1$ and 2 undergo ferroelectric-paraelectric phase transition of diffuse type at $283, 305$ and 320 K respectively. The reason for broadening of the dielectric peak may be due to non-homogeneous distribution of the cations (i.e., substitutional disorder) and defects present in the system [14]. The broadened dielectric peaks in these compounds indicate that the transition is of diffuse type. A particular temperature in broadened dielectric peak cannot be regarded as a definite Curie point rather than a region called Curie region is to be considered [14]. Similar diffusive characteristic has been observed in some other members of the TB-type structure [8–12]. It was also found that the transition temperature shifts towards higher temperature side as the Zr^{+4} concentration increases. The value of ϵ also decreases with increasing Zr^{+4} concentration and at T_c , ϵ is $531, 375$ and 275 for $x = 0, 1$ and 2 respectively. The variation of $\tan \delta$ with temperature of all the compounds shows the same trend. The $\tan \delta$ increases with increasing Zr concentration. The change in the values of $\tan \delta$ of all the

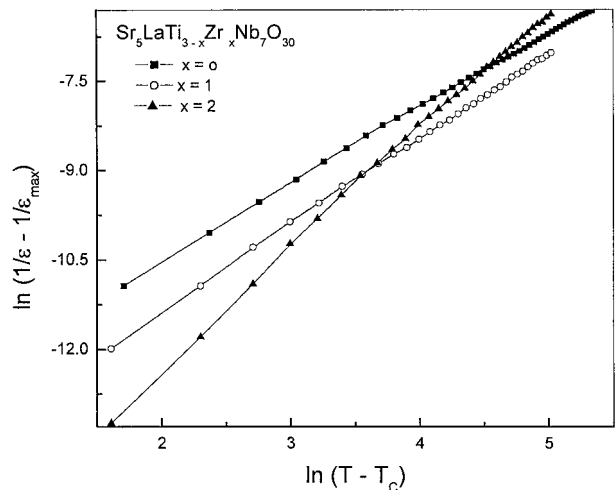


Figure 5 Variation of $\ln(1/\epsilon - 1/\epsilon_{\max})$ vs. $\ln(T - T_c)$ in $\text{Sr}_5\text{LaTi}_{3-x}\text{Zr}_x\text{Nb}_7\text{O}_{30}$ ($x = 0, 1, 2$ and 3).

compounds was considerably less at low temperature. At higher temperature $\tan \delta$ increases considerably. In the paraelectric phase the ferroelectric domain wall's contribution to the $\tan \delta$ diminishes. At higher temperature conductivity begins to dominate resulting in an increase of $\tan \delta$ [15].

The degree of disordering of the compounds was estimated using an empirical relation $(1/\epsilon - 1/\epsilon_{\max}) \propto (T - T_c)^\gamma$ [16], where exponent γ is a measure of diffuseness or disordering of the system. The logarithmic plot related to this equation is shown in Fig. 5. The value of γ was estimated from the slope of $\ln(1/\epsilon - 1/\epsilon_{\max})$ vs. $\ln(T - T_c)$ plot and the calculated values are given in Table I. As the compound with $x = 3$ does not have any dielectric peak, the diffusivity γ not has been calculated. The value of γ is usually 1 obeying Curie-Weiss law and is 2 for completely disordered system. The estimated value of γ for these systems indicates that the materials have strong evidence of diffuse phase transition.

An alternative statistical approach was also used to estimate the degree of disorderness or diffuseness using the relation $\ln(\epsilon_{\max}/\epsilon) = (T - T_c)^2/2\delta_g^2$ [17], where δ_g is Gaussian diffuseness. The plot of $\ln(\epsilon_{\max}/\epsilon)$ vs. $(T - T_c)^2$ is as shown in Fig. 6. The evaluated value of δ_g was given in Table I.

3.3. Electrical properties: impedance study

Impedance spectroscopy was used to study the electrical properties of all the compounds. Polycrystalline materials have variety of frequency dependent effects associated with heterogeneities. One of the advantages of frequency dependent measurements is that the contributions of the bulk material, the grain boundaries and electrode effects can easily be separated if the time constants are different enough [18] to allow separation. The frequency dependent properties of a material can be described via the complex permittivity (ϵ^*), complex impedance (Z^*) and dielectric loss or dissipation factor ($\tan \delta$). These parameters are related to each other in the

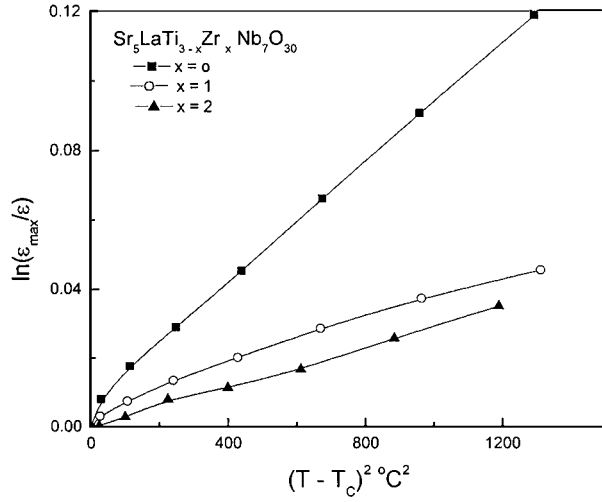


Figure 6 Variation of $\ln(\epsilon_{\max}/\epsilon)$ vs. $(T - T_c)^2$ in $\text{Sr}_5\text{LaTi}_{3-x}\text{Zr}_x\text{Nb}_7\text{O}_{30}$ ($x = 0, 1, 2$ and 3).

following form:

$$Z^* = Z' - jZ'' = \frac{1}{jC_0\epsilon^*\omega}, \epsilon^* = \epsilon' - j\epsilon'' \text{ and}$$

$$\tan \delta = \frac{\epsilon''}{\epsilon'} = \frac{M''}{M'} = \frac{Z'}{Z''} = \frac{Y'}{Y''},$$

where $\omega = 2\pi f$ is the angular frequency ($f =$ frequency), C_0 is the geometrical capacitance, $j = \sqrt{-1}$. These relations offer a wide scope for a graphical analysis of the various parameters under different conditions (i.e., temperature, frequency, etc.).

The relation between Z' (real part of the impedance) and Z'' (imaginary part of impedance) at a representative temperature (673 K) is shown in Fig. 7 for $x = 0, 1, 2$ and 3 . A single semicircular arc with a single relaxation process has been observed in all the cases. As reported in $\text{SrBi}_2\text{Ta}_2\text{O}_9$ or $\text{Na}_{0.5}\text{Bi}_{0.5}\text{TiO}_3$ [19–20], the single semicircular arc confirms that the impedance contribution is mainly due to the grains. As the Zr concentration increases the intercept along the Z' axis shift

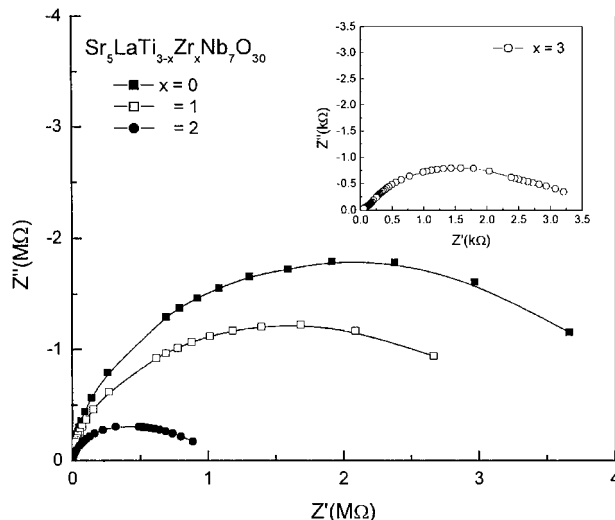


Figure 7 Variation of Z' and Z'' at 673 K in $\text{Sr}_5\text{LaTi}_{3-x}\text{Zr}_x\text{Nb}_7\text{O}_{30}$ ($x = 0, 1, 2$ and 3).

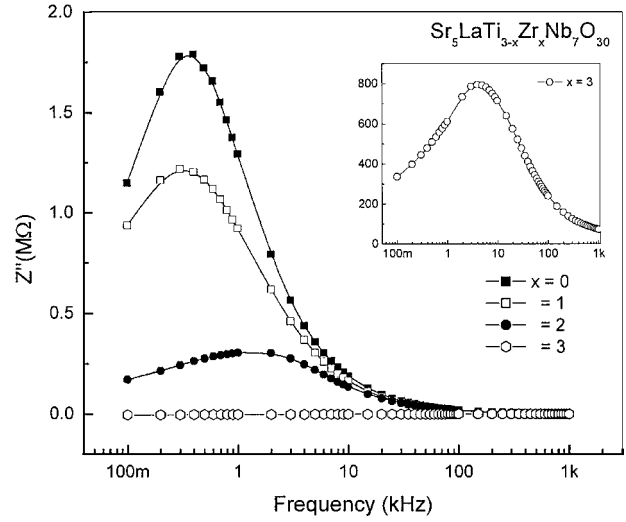


Figure 8 Variation of Z'' vs. $\log(f)$ at 673 K in $\text{Sr}_5\text{LaTi}_{3-x}\text{Zr}_x\text{Nb}_7\text{O}_{30}$ ($x = 0, 1, 2$ and 3).

towards lower values, indicating the reduction in the grain resistance and a possible enhancement in the bulk conduction. The intercept of the semicircular arc on Z' axis has been used to evaluate the bulk resistance (R_b), while the frequency corresponding to Z''_{\max} has been used to evaluate the angular frequency ω .

The variation of Z'' with log of frequency is shown in Fig. 8 at a representative temperature (673 K) for $x = 0, 1, 2$ and 3 . The peak position shifts towards higher frequency and the magnitude of Z'' decreases with increase in the concentration of Zr^{4+} cations. The shift in the peak position towards higher frequency may be due to the reduction in the bulk resistance. The relaxation species may be electrons at low temperature and defects/vacancies at higher temperature that may be responsible for electrical conduction in the material. In relaxation system, one can determine the most probable relaxation time (τ) from the position of the loss peak in the Z'' versus frequency plots using the relation $\tau = R_b C_b = \frac{1}{\omega}$. The τ -value is found to be decreasing as temperature increases showing a typical semiconductor behavior. The variation of τ as a function of temperature implies that the relaxation process is temperature dependent.

The real and imaginary part of the relative dielectric permittivity (ϵ' and ϵ'' respectively) were calculated from Z' and Z'' impedance values using the expressions [21]

$$\epsilon'(\omega) = \left(\frac{g \cdot f}{\omega \epsilon_0} \right) \frac{Z''}{(Z')^2 + (Z'')^2} \text{ and}$$

$$\epsilon''(\omega) = \left(\frac{g \cdot f}{\omega \epsilon_0} \right) \frac{Z'}{(Z')^2 + (Z'')^2},$$

where $g \cdot f$ is the geometrical factor (t/A , t thickness and A the area of the pellet), ϵ_0 the permittivity for free space (8.854×10^{-14} F cm^{-1}). The temperature dependence of (a) ϵ' and (b) ϵ'' at 10 kHz frequency is shown in Fig. 9. The ϵ' decreases for $x = 0$ and 1 whereas for $x = 2$ it has peak at 323 K and it increases continuously for $x = 3$. They were in good agreement

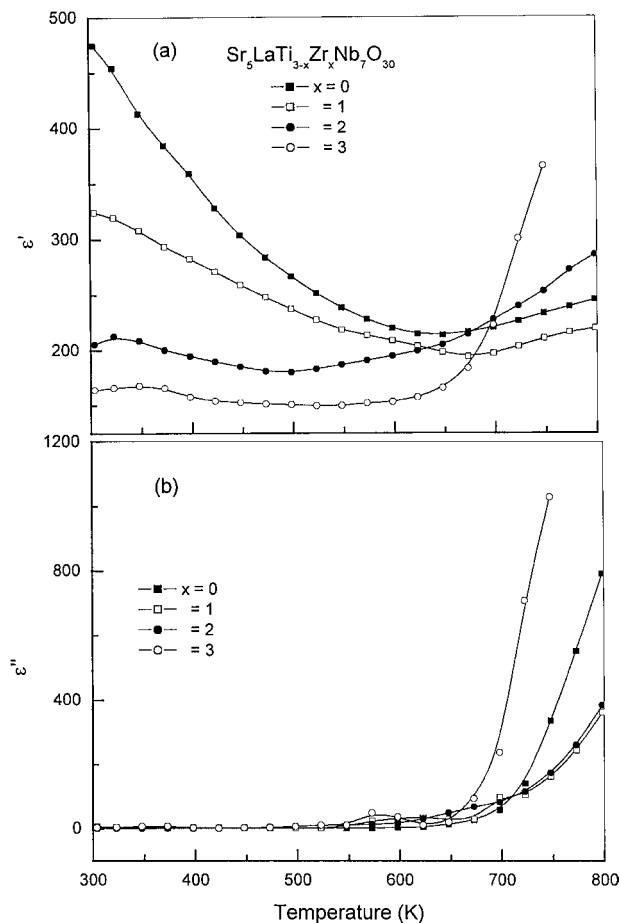


Figure 9 Temperature dependence of (a) ϵ' and (b) ϵ'' at 10 kHz in $\text{Sr}_5\text{LaTi}_{3-x}\text{Zr}_x\text{Nb}_7\text{O}_{30}$ ($x = 0, 1, 2$ and 3).

with dielectric measurement of the compounds, where T_c for $x = 0$ and 1 is below the room temperature (i.e., 283 and 305 K). For $x = 2$ T_c was found to be 320 K. The compound with $x = 3$ does not have any dielectric anomaly in the measured temperature range. The variation of ϵ'' with rise in temperature is very small up to 650 K and after that it increases in all the compound. Similar behavior in ϵ'' and $\tan \delta$ was found in many ferroelectrics [22, 23].

The dc electrical conductivity (σ_{dc}) has been evaluated from the impedance data using a relation $\sigma_{dc} = \frac{l}{R_b A}$. An Arrhenius plot of σ_{dc} against inverse of absolute temperature is shown in Fig. 10. It follows a typical semiconductor like behavior in accordance with the relation [24, 25], $\sigma_{dc} = \sigma_0 \exp\left[-\frac{E_a}{2kT}\right]$, where σ_0 is the preexponential factor, E_a the experimental activation energy, k the Boltzmann constant and T the absolute temperature. From the graph it was clear that the conduction process might be of mixed type (ionic and electronic). The change in the slope was noticed at around 573 K. The experimental activation energy values are given in Table I. The higher value of activation energy in the higher temperature region can be regarded as due to thermally activated mobility of the charge carriers and hence the conductivity is more in this region. The small value of the activation energy at lower temperature may be due to the electronic nature of conduction process, by electron hopping between the ions of different valences [26].

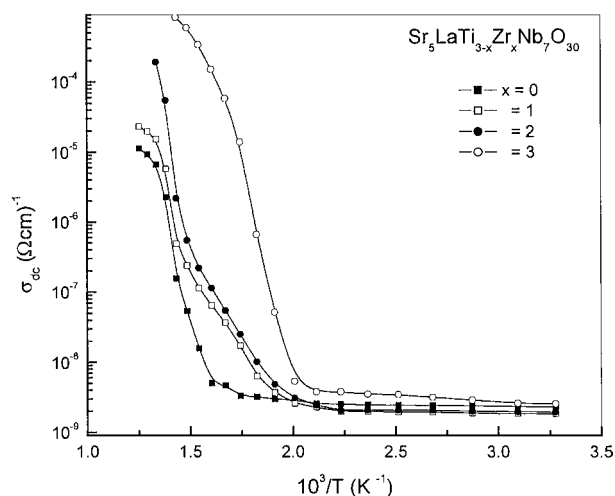


Figure 10 $\log(\sigma_{dc})$ vs. $[10^3/T]$ in $\text{Sr}_5\text{LaTi}_{3-x}\text{Zr}_x\text{Nb}_7\text{O}_{30}$ ($x = 0, 1, 2$ and 3).

4. Conclusion

In spite of some similarities in the crystal parameters of the compounds prepared by high temperature solid-state reaction technique, there is a marked difference in their physical properties. All the compounds have orthorhombic crystal structure even after complete substitution of Zr^{+4} at the Ti^{+4} site. All the compounds, except $x = 3$ show diffuse phase transition. The T_c shifts towards higher temperature as x increases. We, also observed that as x increases the diffusivity increases. All the compounds exhibit negative temperature coefficient of resistivity, which indicates the intrinsic semiconductor property of the materials.

References

1. B. WUL and L. M. GOLDMAN, *C. R. Acad. Sci. URSS* **46** (1945) 139.
2. J. C. TOLEDANO, *Phys. Rev. B* **12**(3) (1975) 943.
3. K. MEGUMI, N. NAGATSUMA, Y. KASHIWADW and Y. FURUHATA, *J. Mater. Sci.* **11** (1976) 1583.
4. R. R. NEUGAONKAR, W. KCORY, W. W. HO and W. F. HALL, *Ferroelectrics* **38** (1981) 857.
5. V. HORNEBECQ, C. ELISSALDE, V. POROKHONSKYY, V. BOVTUN, J. PETZELT, I. GREGARA and M. MAGLIONE, *J. Phys. Chem. Solids* **64** (2003) 471.
6. HITOSHI and M. IMAEDA, *Mats. Chem. Phys.* **79** (2003) 199.
7. M.-SUP KIM, P. WANG, J.-HYUNG LEE, J.-J. KIM, H. Y. LEE and S.-H. CHO, *Jpn. J. Appl. Phys.* **41** (2002) 7042.
8. X. H. ZHENG and X. M. CHEN, *J. Mater. Res.* **17** (2002) 1664.
9. S. R. SHANNIGRAHI, R. N. P. CHOUDHARY, A. KUMAR and H. N. ACHARYA, *J. Phys. Chem. Solids* **59** (1998) 737.
10. R. PALAI, R. N. P. CHOUDHARY and H. S. TEWARI, *ibid.* **62** (2001) 695.
11. N. K. SINGH, R. N. P. CHOUDHARY and A. PANIGRAHI, *Mater. Chem. Phys.* **74** (2002) 113.
12. X. H. ZHENG and X. M. CHEN, *Solid State Communications* **125** (2003) 449.
13. E. WU, "POWDER", an Interactive Powder Diffraction Data Interpretation and Indexing Programme, Ver. 2.1, School of Physical Science, Flinders University of South Australia, Bedford Park, S. A., 5042, Australia.
14. M. E. LINES and A. M. GLASS, *Principles and Applications of Ferroelectrics and Related Materials* (Oxford Univ. Press, 1977).

15. S. KU HARUANGRONG, *J. Mater. Sci.* **36** (2001) 1727.
16. S. M. PILIGRIM, A. E. SUTHERLAND and S. R. WINZER, *J. Amer. Ceram. Soc.* **73** (1990) 3122.
17. S. MIGA and K. WOJEIK, *Ferroelectrics* **100** (1987) 167.
18. J. R. MACDONALD, "Impedance Spectroscopy" (Wiley, New York, 1987).
19. A. R. JAMES and K. SRINIVAS, *Mater. Res. Bull.* **34** (1999) 1301.
20. Y. WU, M. J. FORBES, S. SERAJI, S. J. LIMMER, T. P. CHOU and G. CAO, *Mater. Sci. Engg. B* **86** (2001) 70.
21. A. P. BARRANCO, F. C. PINAR, O. P. MARTINEZ, J. DE L. S. GUERRA and I. G. CARMENATE, *J. Euro. Ceram. Soc.* **19** (1999) 2677.
22. P. PRABHAKAR RAO, S. K. GHOSH and P. KOSHY, *J. Matls. Sci. Matls Electron.* **12** (2001) 729.
23. M.-S. KIM, J.-H. LEE, J.-J. KIM, H. Y. LEE and S.-H. CHO, *J. Euro. Ceram. Soc.* **22** (2002) 2107.
24. Y. M. GUREVICH, "Electric Conductivity of Ferroelectrics," Moskva, 1969.
25. W. D. KINGERY, "Introduction to Ceramics," 2nd ed., (Wiley, New York, 1976).
26. M. A. AHMED, ATEIA, S. I. EI-DEK and F. M. SALEM, *J. Mater. Sci.* **38** (2003) 1087.

*Received 2 October 2002
and accepted 13 October 2003*